Supporting information (SI) of manuscript

Palladium recovery in a H_2-based membrane biofilm reactor: formation of Pd(0) nanoparticles through enzymatic and autocatalytic reductions

Chen Zhou[1]*, Aura Ontiveros-Valencia[1], Zhaocheng Wang[1,2], Juan Maldonado[1], He-Ping Zhao[3], Rosa Krajmalnik-Brown[1], and Bruce E. Rittmann[1]

[1]Swette Center for Environmental Biotechnology, Biodesign Institute, Arizona State University, USA

[2]Department of Water Engineering and Science, College of Civil Engineering, Hunan University, China

[3]Department of Environmental Engineering, College of Environmental and Resource Sciences, Zhejiang University, Hangzhou, China

*Corresponding author

Present address: Swette Center for Environmental Biotechnology, Biodesign Institute, Arizona State University, Tempe, AZ 85207-5701, USA

Tel: +01-480-217-3742

Email: zhou_SCEB@asu.edu

Summary of SI:

- Pages: 11
- Tables: 1
- Figures 8

Tables

Table S1. Genus-level abundances of the biofilms at all three stages. For each genus, the most abundant stage is indicated by the abundance numbers with the **bold Bernard MT** font.

Taxonomic rank					Abundance		
PHYLUM	CLASS	ORDER	FAMILY	GENUS	Stage 0	Stage ~~1~~ 1	Stage ~~1~~ 2
Euryarchaeota	Methanobacteria	Methanobacteriales	Methanobacteriaceae	*Unclassified*	0.768%	0.175%	**1.707%**
				Methanobacterium	0.100%	0.000%	**1.000%**
				Methanobrevibacter	0.000%	0.000%	**0.129%**
Actinobacteria	Actinobacteria	Actinomycetales	Mycobacteriaceae	***Mycobacterium***	0.043%	**32.775%**	1.971%
Bacteroidetes	Flavobacteriia	Flavobacteriales	Weeksellaceae	***Chryseobacterium***	**3.011%**	0.000%	2.182%
Proteobacteria	α-proteobacteria	Rhizobiales	Bradyrhizobiaceae	*Unclassified*	0.318%	**10.143%**	1.739%
			Hyphomicrobiaceae	*Unclassified*	0.100%	0.000%	**2.161%**
		Rhodospirillales	Rhodospirillaceae	*Unclassified*	0.136%	**2.921%**	0.464%
	β-proteobacteria	Burkholderiales	Comamonadaceae	*Unclassified I*	0.643%	**10.221%**	7.182%
				Unclassified II	1.943%	**12.232%**	1.550%
		Rhodocyclales	Rhodocyclaceae	*Unclassified*	2.546%	**2.818%**	1.457%
				Dechloromonas	**61.643%**	4.382%	39.157%
				Dok59	2.350%	0.518%	**2.621%**
				Thauera	**2.986%**	0.004%	0.489%
	δ-proteobacteria	Desulfovibrionales	Desulfovibrionaceae	***Desulfovibrio***	1.443%	**8.689%**	0.061%

SI Figures

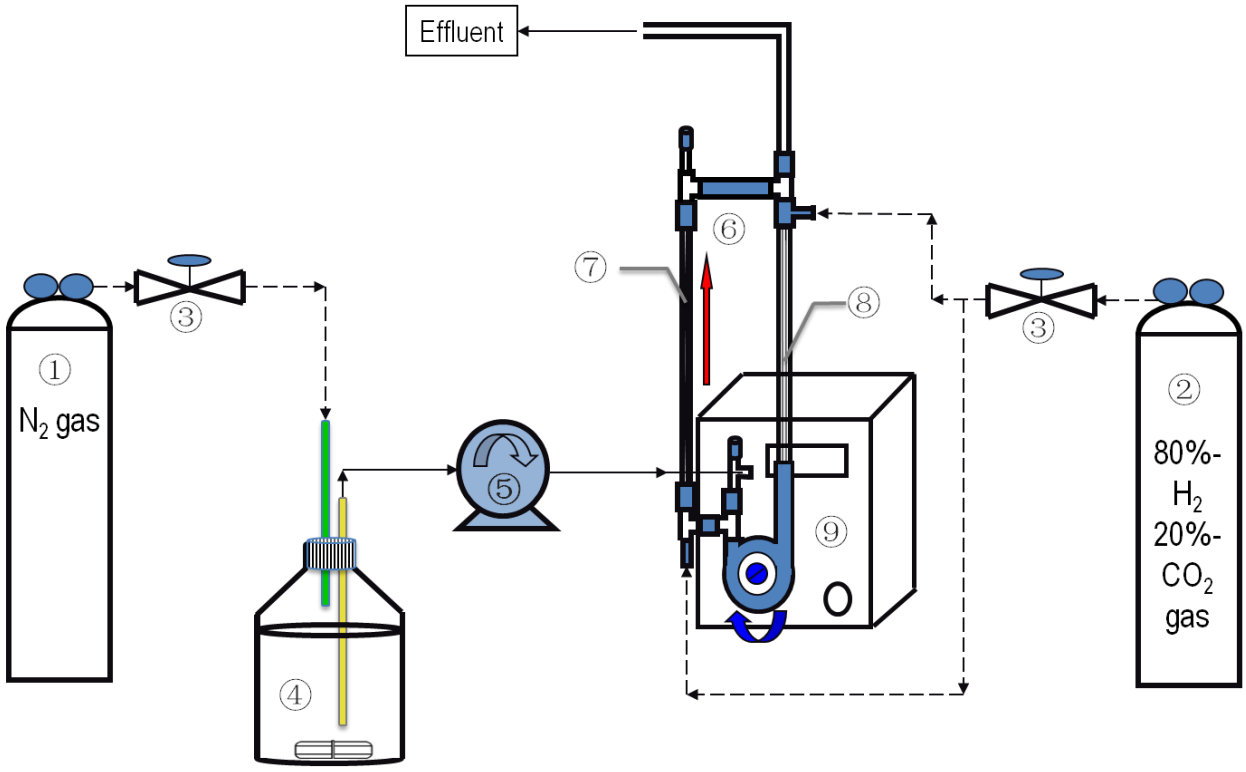

Fig S1. Schematic of the bench-scale MBfR system used to investigate Pd recovery. The major components include: ① pure N_2 gas to feed the headspace of the medium bottle; ② mixed gas tank with 80% H_2 and 20% CO_2 gas tank to feed the fiber bundles of the MBfR; ③ gas pressure regulators; ④ Pd medium bottle with a stir bar; ⑤ feeding pump; ⑥ MBfR configuration (the red arrow indicates the flow direction; ⑦ main bundle with 50 fibers; ⑧ biofilm sampling bundle with 10 coupon fibers; ⑨ recirculation pump. The black solid arrows indicate the liquid flow, and the black dashed arrows indicate the gas flow.

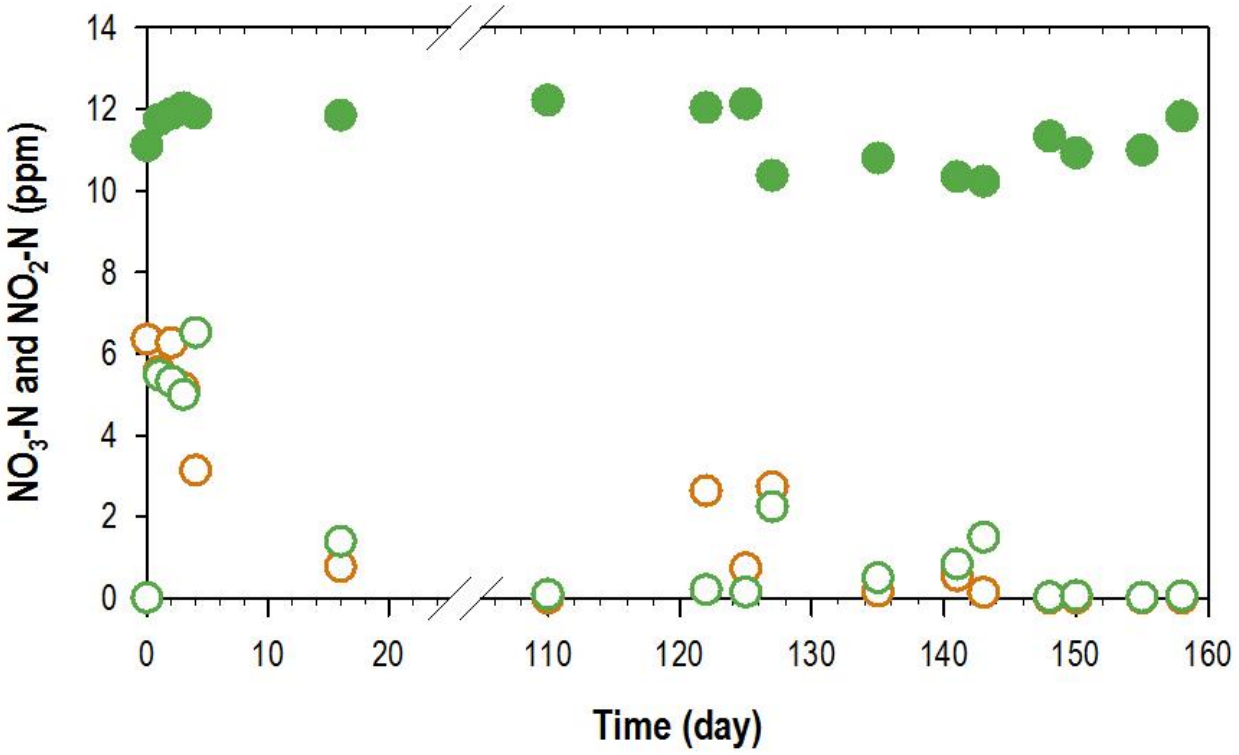

Fig S2. Nitrate and nitrite profiles in Stage 0. Solid green circles: nitrate concentrations in influent. Empty green circles: nitrate concentrations in effluent. Empty brown circles: nitrite concentrations in effluent. Nitrite was absent in the influent.

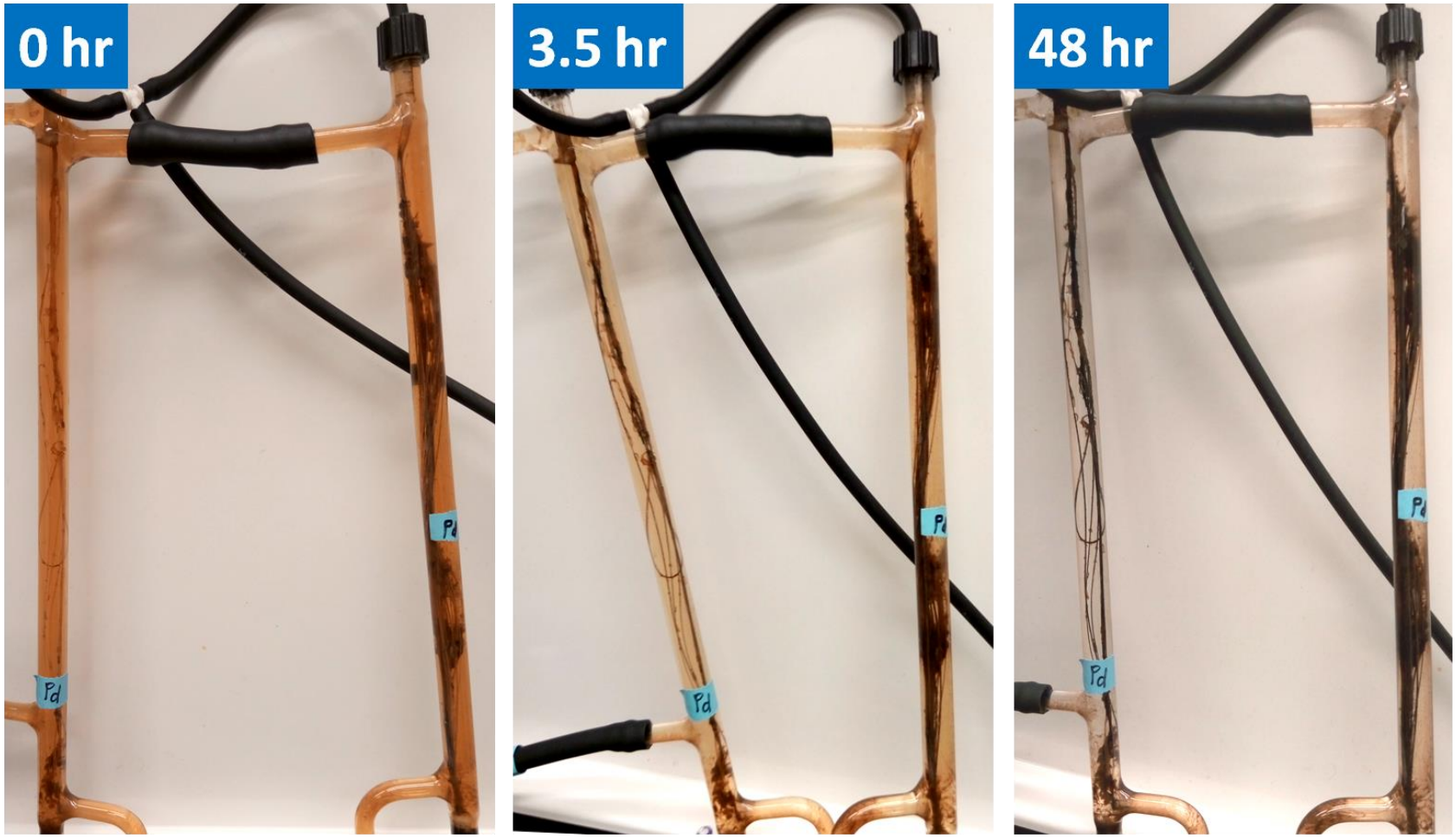

Fig S3. Photos of the MBfR taken immediately, 3.5 hours, and 48 hours after we primed it with Pd-containing medium. The liquid color lightening along time indicates Pd recovery, and the fiber surface darkening (especially observable on the coupon fiber bundle on the left side) indicates Pd precipitation.

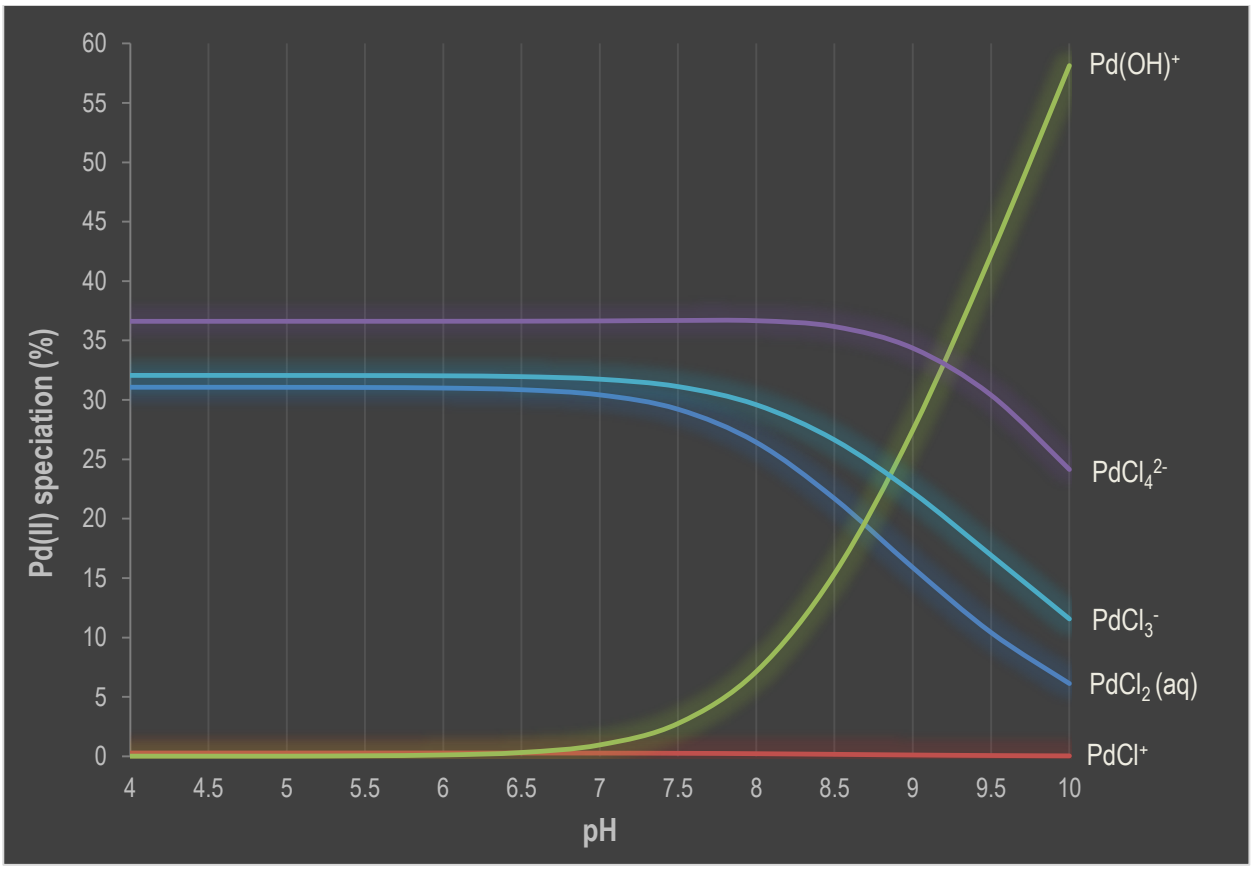

Fig S4. Pd(II) speciation as a function of pH computed by Visual MINTEQ, with the default values being $[Pd(II)]_{total}$ = 0.002 M, $[Cl^-]_{total}$ = 0.01 M, ionic strength (I) = 0.03 M, and temperature (T) = 22°C.

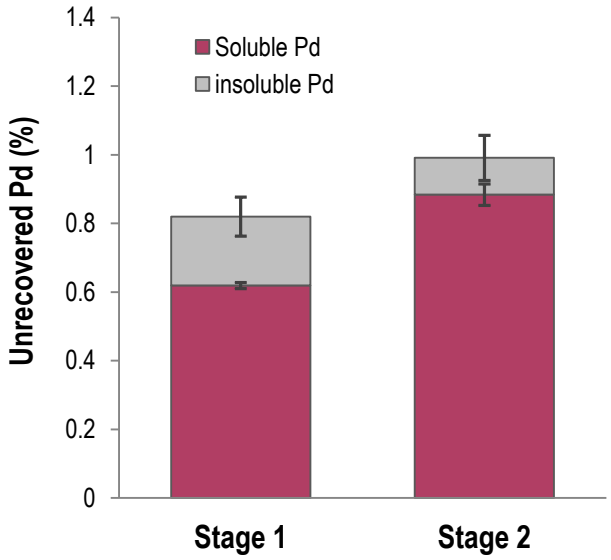

Fig S5. The average percentages of unrecovered Pd in the effluents at Stages 1 and 2. The measured Pd concentrations in the filtered and unfiltered liquid samples refer to the soluble and total Pd concentrations, respectively. The insoluble Pd concentration were calculated by subtracting the soluble Pd concentration from the total Pd concentration.

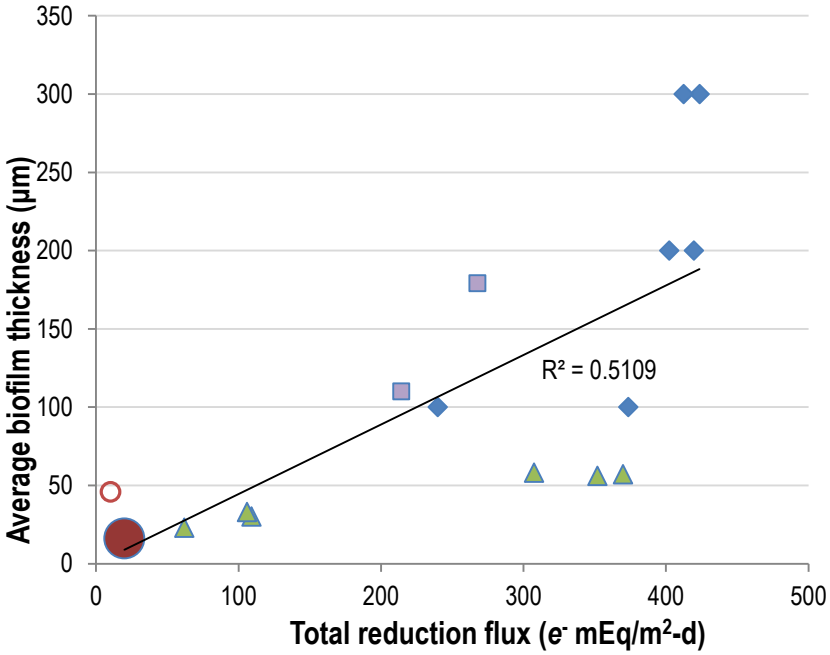

Fig S6. Correlation of total reduction flux versus average biofilm thickness on basis of experimental or modeling data from a denitrifying MBfR[1] (purple squares), a nitrate- and perchlorate-reducing MBfR[2] (green triangles), a nitrate- and sulfate-reducing MBfR[3] (blue diamonds), a U(VI)-reducing MBfR[4] (small empty circle), and the Pd(II)-reducing MBfR in this study (big filled circle).

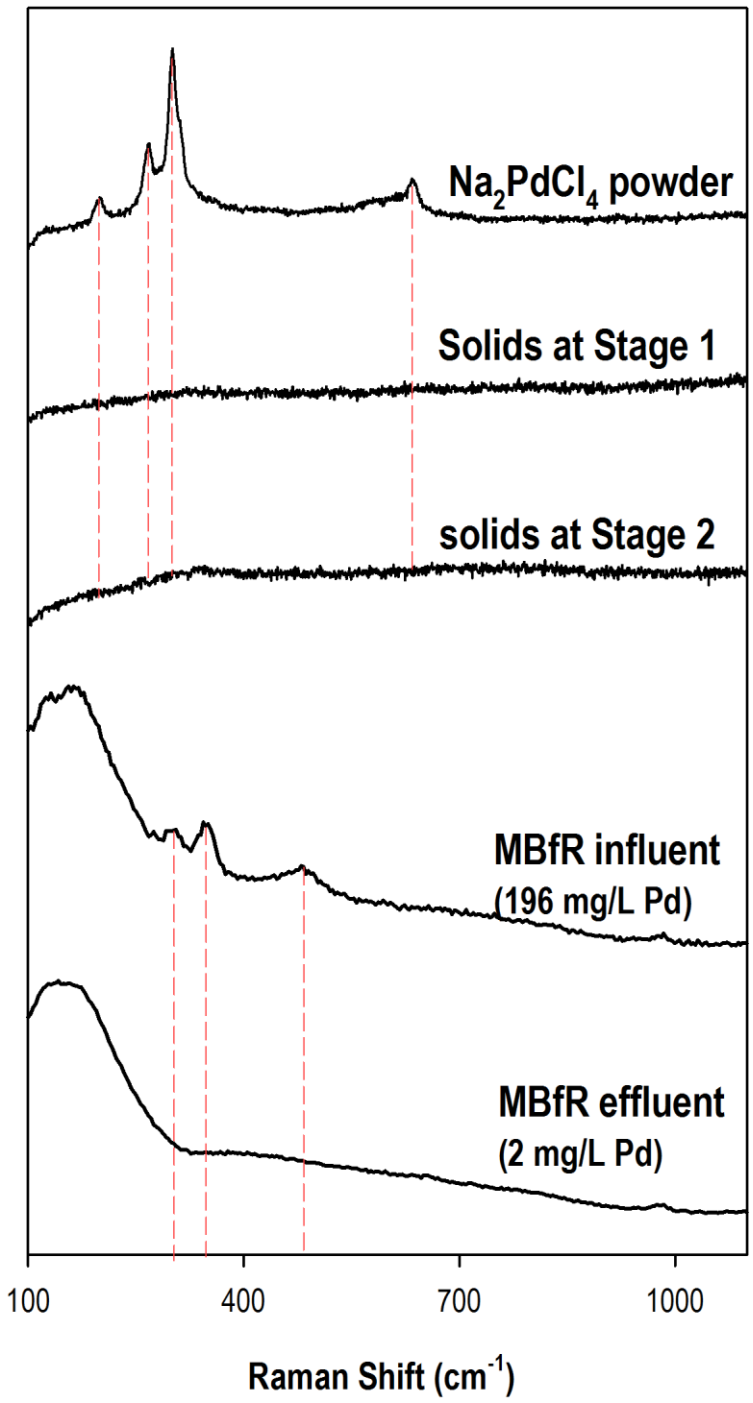

Fig S7. Raman spectra of the original and final Pd solids at Stages 1 and 2, as well as the influent and effluent liquid.

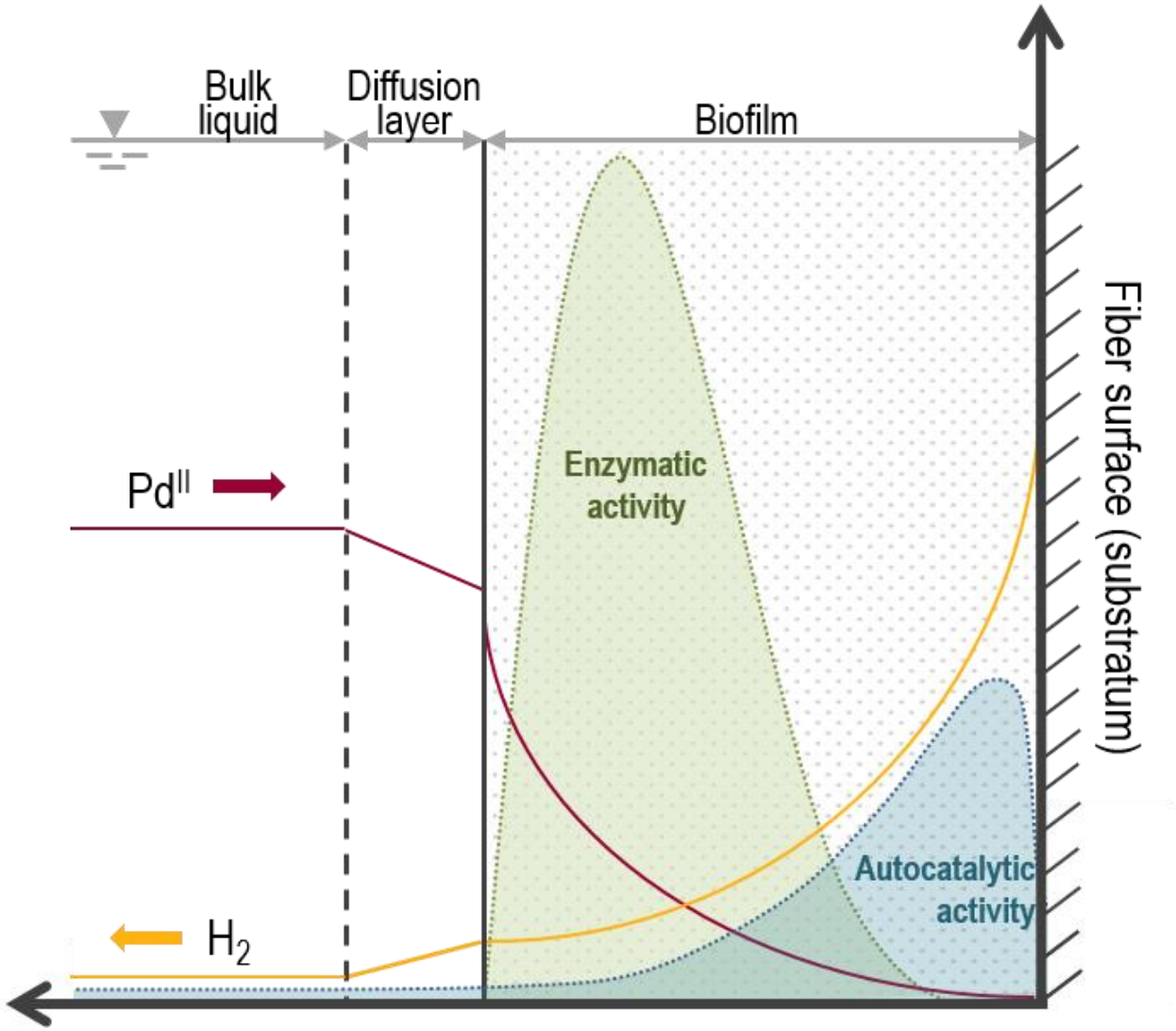

Fig S8. Proposed gradient profile of substrate concentrations and reaction activities in the Pd(II)-reducing MBfR.

References in SI

1. Lee, K. C.; Rittmann, B. E., Applying a novel autohydrogenotrophic hollow-fiber membrane biofilm reactor for denitrification of drinking water. *Water Res* **2002,** *36*, (8), 2040-2052.
2. Tang, Y. N.; Zhao, H. P.; Marcus, A. K.; Krajmalnik-Brown, R.; Bruce, E. R., A steady-state biofilm model for simultaneous reduction of nitrate and perchlorate, part 2: parameter optimization and results and discussion. *Environ Sci Technol* **2012,** *46*, (3), 1608-1615.
3. Martin, K. J.; Picioreanu, C.; Nerenberg, R., Assessing microbial competition in a hydrogen-based membrane biofilm reactor (MBfR) using multidimensional modeling. *Biotechnol Bioeng* **2015**.
4. Zhou, C.; Ontiveros-Valencia, A.; Cornette de Saint Cyr, L.; Zevin, A. S.; Carey, S. E.; Krajmalnik-Brown, R.; Rittmann, B. E., Uranium removal and microbial community in a H_2-based membrane biofilm reactor. *Water Res* **2014**.